

Lawrence Berkeley National Laboratory

Lawrence Berkeley National Laboratory

Title

DESIGN FEATURES AND OPERATIONAL CHARACTERISTICS OF THE PEP
BEAM-TRANSPORT AND INJECTION SYSTEM

Permalink

<https://escholarship.org/uc/item/49k660mb>

Author

Peterson, J.M.

Publication Date

1981-03-01

Peer reviewed

MASTER

LBL-11742

CONF 810314-1120

Lawrence Berkeley Laboratory

UNIVERSITY OF CALIFORNIA

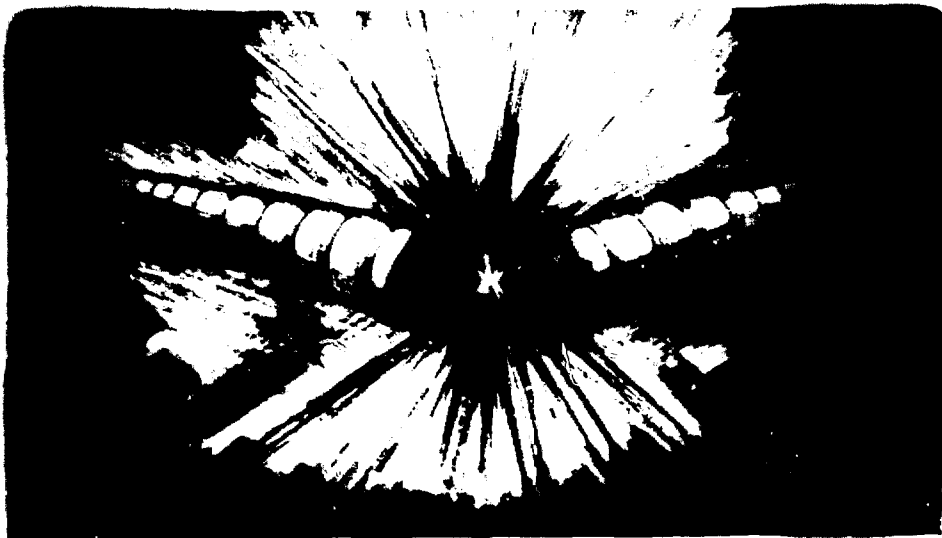
Accelerator & Fusion Research Division

Presented at the IEEE Particle Accelerator
Conference, Washington, D.C., March 11-13, 1981

DESIGN FEATURES AND OPERATIONAL CHARACTERISTICS
OF THE PEP BEAM-TRANSPORT AND INJECTION SYSTEM

J.M. Peterson, K.L. Brown, and J.B. Truher

March 1981



APPROVED FOR THIS PROJECT IS GRANTED

DESIGN FEATURES AND OPERATIONAL CHARACTERISTICS OF THE PEP BEAM-TRANSPORT AND INJECTION SYSTEM

J.M. Peterson*
Lawrence Berkeley Laboratory
University of California
Berkeley, California 94720

K.L. Brown**, J.B. Truher**
Stanford Linear Accelerator Center
P.O. Box 4349
Stanford, California 94305

Summary

The PEP beam-transport system was designed to transmit 4-to-15 GeV electron and positron beams from the SLAC linac within a ± 0.8 percent momentum band, to have flexible tuning of the betatron and off-momentum functions for matching into the PEP storage ring, and to have convenient operating characteristics. The transport lines were brought into operation quickly and have operated well. Electron injection has been consistent and efficient and relatively easy to accomplish. Positron injection also has been satisfactory but is variable and more sensitive to ring conditions.

The Beam-Transport System

The PEP beam-transport and injection system^{1,2,3} has two beam-transport lines, which conduct the electron and positron beams from the Stanford two-mile linear accelerator to the two injection regions in the PEP ring. Each injection region has a system of "bump" and "kicker" magnets that launches the beam onto a suitable orbit within the vacuum chamber of the ring. The arrangement of the transport line, the optical properties, the instrumentation, and the control elements are schematically shown in Fig. 1.

Those pulses from the linear accelerator that are intended for PEP are switched into the PEP transport lines by pulsed magnets (PM 1,2 in Fig. 1) near the end of the linear accelerator. The waveform of each pulse of the switch magnets is a 600-Hz full-wave sinusoid, whose timing is controlled so as to have the polarity appropriate to the electron or positron beam being switched. The nominal characteristics of the PEP beams delivered to the ring are:

	Electrons	Positrons
Energy	4-15 [†]	4-15 [†] GeV
Energy spread	± 0.15	$\pm 0.3-0.5$ percent
Emittance (at 15 GeV)	0.007	$0.15 \times \text{mm-mrad}$
Pulse length	1	1 nanosecond
Rep. Rate, max	180	180 pps
Intensity	10^9	2×10^8 per pulse

[†] The magnets of the injection system are capable of 20-GeV operation but are power-supply limited at present to 15 GeV.

The PEP beam pulses are deflected downward by 5.5 milliradians into a horizontal d.c. splitting magnet, which deflects electrons into the north injection

* This work was supported by the Director, Office of Energy Research, Office of High Energy and Nuclear Physics, High Energy Physics Division of the U.S. Department of Energy under Contract No. W-7405-ENG-48.

** This work was supported by the Department of Energy, Contract DE-AC03-76SF00515

line and positrons into the south injection line. Each transport line is made up of a 7000 lattice with 90° betatron phase shift per cell and has a total of three wavelengths. The bend magnets (B1 through B9) required for the 60° of bend in the horizontal plane are arranged in the first and second wavelengths in such a way as to provide an achromatic region in the five-quadrupole section Q6 to Q10, as shown in Figure 1. A small (5.9 milliradian) bend magnet (BVA) is inserted between quadrupoles Q2 and Q3 to correct the vertical dispersion created by the pulsed switching magnet. The elevation of the PEP ring is 11.16 meters below the exit point of the linac, which forces the plane of the 60-degree of "horizontal" bend to be tilted 6.1 degrees about the axis of the linac. At quadrupole Q16 the beam is descending with a slope of 83.4 milliradians, but it is returned to horizontal at the exit of the Lambertson septum magnet B11, where it is launched into the storage ring. Equal vertical bends in magnets B10 and B11, separated by 180° in betatron phase, makes the system achromatic at the launch point.

The interquad spacing is 8.50 meters up to Q17 and 9.14 meters thereafter. The total length of each transport line, from the pulsed switching magnets to the Lambertson septum magnet is 224 meters.

Transverse and Longitudinal Phase-Space Matching

The achromatic region that includes Q6 through Q10 was provided so that these five quadrupoles could be used to match the beam emittance to the acceptance of a range of ring lattices without affecting the dispersion properties of the transport line. Computer modeling showed that a satisfactory match into all of the anticipated ring lattices can be made with this arrangement. This matching of the transverse phase space was expected to be useful principally for the positron beam, whose emittance is relatively large. However, matching can benefit the electron line as well in that it allows good injection efficiency over a wider range of steering conditions in the linac and in the line.

Independent matching of the magnitude and slope of the horizontal dispersion function also is possible in the transport line. The launch point was chosen to be a point where the dispersion function η of the ring was approximately zero for all of the lattices under consideration. However, the slope η' at this point was finite for several of the lattices and thus required matching, at least for the positron beam, whose momentum width is ± 0.3 percent or more. Although not required for electron injection, η' -matching benefits it as well in that it allows good efficiency over a wider range of energy settings in the linac. Matching of the slope of the horizontal dispersion function can be accomplished by simultaneous tuning of Q13 and Q17. Q13 is in a high dispersion region and thus it can produce momentum-dependent steering. Since it is 3 $\lambda/2$ upstream from the launch

point, it affects n' but not n at that point. Q17 is at point of zero dispersion $\lambda/2$ downstream from Q13 and thus can compensate the change in transverse phase space produced by Q13 without affecting the dispersion function. The required excitation change in Q17 is equal and opposite to that of Q13. In this way, n' -matching can be accomplished without affecting the transverse phase space.

Matching from the Linac to the Transport Line

The focusing of the beams in the two-mile linac is achieved by doublet quadrupole magnets at 100-meter intervals, and normally the betatron functions vary between 36 and 163 meters. In order to match the transport lattice, whose betatron functions vary between 5.0 and 30 meters, three pulsed quadrupole magnets (PQ1, PQ2, and PQ3 in Figure 1) were inserted in the available 6-inch gaps that occur at 40-foot intervals in the linac accelerating structure. With this number of quadrupole magnets and the restricted spacings available, only an approximate match is obtained into the transport line. Since the doublet quadrupoles in the linac have fixed polarity, the matching conditions for electron beams are different from those for positron beams.

The Quadrupole-Shunt Method of Beam Alignment

The quadrupole-shunt method of beam alignment uses the feature that if the beam is not centered in a quadrupole magnet, changing the excitation in that quadrupole will produce steering of the beam that can generally be observed at a downstream scintillator screen (other than one located at $n\pi$ phase shift from that quadrupole). If each quadrupole can be independently varied, a small number of beam-position monitors can suffice to indicate the position of the beam center in a large number of quadrupole magnets. In the PEP beam-transport lines, most of the quadrupole magnets are in series circuits so that in order to provide independent variation, the individual magnets were fitted with resistive shunts that temporarily reduce the excitation current by a factor of two on command from the control room. The resultant shift Δx_j (in the horizontal plane, e.g.) of the beam center at the beam monitor at position j due to the beam's being off center by the amount Δx_i in the quadrupole at point i in this case is

$$\Delta x_j = * \Delta x_i S_{ij} / 2f_i$$

where f_i is the focal length of the quadrupole ($B_0/B'L_i$), S_{ij} is the sine-like transport function (the M_{12} transfer matrix element) between points i and j , and the sign is + for the focusing plane and - for the defocusing plane. In the PEP beam-transport lines, f_i is 6.0 meters for most of the line (6.5 meters in the last wavelength), S_{ij} is a maximum of about 30 mm/mrad for the focusing plane case and 8.5 mm/mrad for the defocusing plane. Thus for a 1-mm error in the beam center at a quadrupole, the observed shift in beam position at a downstream monitor due to the shunt at that quadrupole can be up to 2.5 mm in the focusing plane or 0.7 mm in the defocusing plane. Since this steering effect is much stronger in the focusing plane, it is usually sufficient to use only the focusing quadrupoles when checking or correcting the steering in a given plane.

The Inflection System

Injection into the PEP storage ring is accomplished by launching each incident beam pulse on a horizontal collective oscillation in such a way that the beams already stored are not disturbed. Radiation damping during the inter-pulse feeding interval allows each

pulse to be injected without harm to the preceding pulse. The phase-space situation is illustrated in Figure 2.

The amplitude and angle of the launch trajectory are controlled by beam "bumps" - i.e., local distortions of the closed orbit. See Figure 3. A fast bump, produced by a set of three kicker magnets, serves to pull the injection orbit away from the septa before the injected pulse makes one revolution of the storage ring. The kicker pulse rises and falls within about two-thirds of a revolution, so that only one of the three bunches of each stored beam is appreciably affected. The three kicker magnets are electrically connected in series, so that the quality of the bump cannot be inadvertently affected by changes in kicker excitation. The d.c. beam bump, which is produced by four independently powered d.c. bend magnets, serves to bias the amplitude and angle of the closed orbit at the launch point during the injection period. The d.c. bump is needed in addition to the fast bump because the septa have to be positioned outside the beam "stay-clear" boundary (10 standard widths of the damped stored beam plus 1 cm), which requires the total bump to be considerably larger than the minimum kicker bump. A single large kicker bump would have been sufficient, but it would have been considerably more expensive as well as more difficult to provide.

Operational Experience with the Beam-Transport And Injection Systems

Both beam-transport lines were brought into operation quickly and without undue difficulty. The quadrupole-shunt method of beam alignment proved to be a valuable technique. Using this method the first beams were quickly and systematically steered down each transport line. This technique is in daily use for diagnosing and adjusting the steering of the beams. There has been no indication of misalignment in any part of the transport system.

The focusing of the beam agrees very well with theory. The spot sizes and shapes are essentially those calculated by the TRANSPORT code at all ten of the scintillation screens in each line. In the achromatic sections of the line the position of the beam spots will stay fixed until fading occurs as the linac energy is varied.

The transmission efficiency of the electron transport line is nearly 100 percent (within 10 percent instrumental uncertainty). In the positron line about half the beam is lost in the first region of high dispersion, which is consistent with the known energy distribution of the positron beam and the aperture and dispersion in the line. Beyond this point the transmission of the positron beam also is essentially 100 percent.

In each transport line there is a scintillator screen at a point of high dispersion to display the energy spread in the beam. At high beam intensity this screen exhibits also beam loading and beam breakup in the linac, as shown in Figure 4. This is the display of one 4-nanosecond electron test-beam pulse of about 75 mA intensity (averaged over the 4ns pulse). The dispersion at this point is about 30 mm/percent, and the high-energy end is at the left. Beam loading in the linac decreases the energy progressively throughout the beam pulse, so that this display in energy is also a display in time in which the S-band microstructure in the beam can be seen. Beam-breakup in both the vertical and horizontal planes also is evident. From pulse to pulse the patterns are similar although they differ in detail.

The emittance- and dispersion-matching features of the transport lines have not yet been explored much beyond that possible with the pulsed quadrupoles. For operational convenience at turn-on, all of the d.c. quadrupoles were put in series circuits, so that the individual variations required for matching are not yet possible. Since adequate injection rates have been achieved without optimum matching, the testing of these features has been delayed.

Operation of the PEP injection systems has been good enough that a thorough testing and analysis has not yet been required. Electron beams are readily stored in the ring, and filling rates up to 25 milliamperes per minute have been recorded. The incident beam sometimes has to be "spoiled" to reduce the electron filling rate to a more convenient level. The injection efficiency for electrons has been estimated to be on the order of 100 percent in some instances, but more typically 40 to 50 percent can be readily obtained.

Satisfactory positron injection has been harder to achieve. Positron filling rates up to 4 milliamperes per minute have been observed, and a rate of 1 to 2 milliamperes per minute can usually be obtained. Positron injection efficiencies up to 70 percent have been recorded, and typically 20 to 40 percent is observed. Positron injection tends to be variable and sensitive to small changes in ring conditions. One possible reason for the greater difficulty with the injection of positrons is the greater energy spread in the incident positron beam coupled with the spurious horizontal and vertical dispersion observed in the ring. This hypothesis has not been adequately tested.

References

1. K. L. Brown, R. T. Avery, and J. M. Peterson, IEEE Trans. Nuc. Sci., NS-22-3, p.1423 (1975).
2. J. M. Peterson and K. L. Brown, IEEE Trans. Nuc. Sci., NS-26-3, p. 3496 (1979).
3. R. Reimers et. al., IEEE Trans. Nuc. Sci., NS-26-3, p. 4027 (1979).

Figure 1: PEP BEAM TRANSPORT LINES INSTRUMENTATION & CONTROL SUMMARY

	PO1	PO2	PO3	PM1,2	Q1	Q2	Q3	Q4	Q5	Q6	Q7	Q8	Q9	Q10	Q11	Q12	Q13	Q14	Q15	Q16	Q17	Q18	Q19	Q20	Q21	Q22	Q23	Q24	INJECT	
TRANSPORT ELEMENTS	LI	LI	LI	LI	Q	Q	Q	Q	Q	Q	Q	Q	Q	Q	Q	Q	Q	Q	Q	Q	Q	Q	Q	Q	Q	Q	Q	Q	Q	
OPTICAL PHASE	0°	0°	0°	0°	0°	90°	180°	270°	360°	0°	90°	180°	270°	360°	0°	90°	180°	270°	360°	0°	90°	180°	270°	360°	0°	90°	180°	270°	360°	
DISPERSION					1%				30mm/%					1%					2 x 360°											
BEND SHUNTS																														
HORIZ. STEERING		✓	✓	✓				✓	✓					✓	✓				✓	✓										
VERT. STEERING	✓				✓			✓	✓					✓	✓				✓	✓										
SCINT - TV PROFILE MONITOR	PM1				PM2					PM3				PM4									PM5	PM6			PM7	PM8	PM9	PM10
QUAD. SHUNTS																														
WALL CURRENT MONITORS	IM1				IM2	IM3								IM4																
TOROID MONITORS					TM1	TM2																								
FARADAY CUP																														
BEAM SLITS		SL1	SL2		SL3																									
BEAM STOPS					BS1					BS2																				
ION CHAMBERS	IC1	IC2	IC3		IC4	IC5				IC6																				

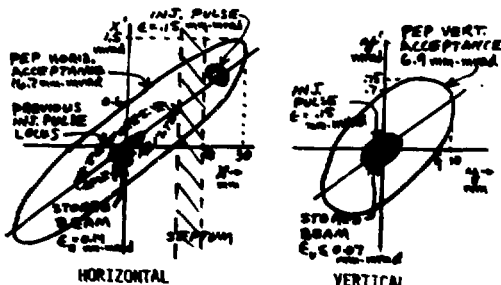


FIGURE 2: INJECTION PHASE SPACE

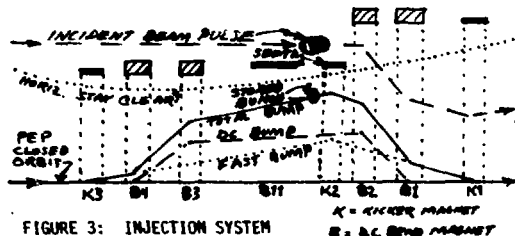


FIGURE 3: INJECTION SYSTEM



FIGURE 4: HIGH-DISPERSION LOSSES OBSERVED AT HIGH-DISPERSION POINT